# Radial properties of the geodesic acoustic mode

Zhenqian Li,[1] Jiaqi Dong,[2,1] Zhengmao Sheng,[1,a)] M. Y. Yu,[1,3] and Weixing Wang[4,b)]

[1)] *Institute for Fusion Theory and Simulation and Department of physics, Zhejiang University, Hangzhou 310027, China*

[2)] *Southwest Institute of Physics, Chengdu 610041, China*

[3)] *Institute for Theoretical Physics I, Ruhr University, Bochum D-44780, Germany*

[4)] *Princeton Plasma Physics Laboratory, Princeton University, P. O. Box 451, Princeton, New Jersey, 08543*

(Dated: 30 March 2017)

In toroidal magnetized plasmas neoclassical effects and drift wave turbulence can induce the geodesic acoustic mode (GAM). We simulate the GAM using the gyrokinetic code GTS with the equilibrium plasma parameters of an experiment. The dynamic properties of the GAM are investigated in detail, in particular its frequency continuum, evolution of its radial wave number, and its propagation characteristics. The simulation results are compared with that from the theoretical models. It is also shown that the GAM radial phase velocity is proportional to the ion thermal speed, as has been found experimentally.

PACS numbers: 52.35.Ra, 52.55.Fa, 52.35.Kt

[a)] zmsheng@zju.edu.cn

[b)] wwang@pppl.gov

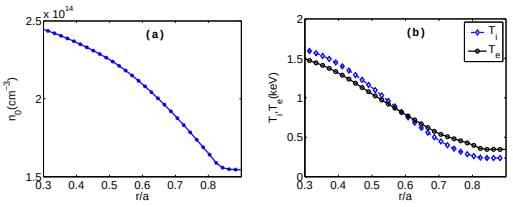


FIG. 1. Initial radial profiles of the (a) electron (or ion) density $n(r)$, and (b) electron ($T_e$) and ion ($T_i$) temperatures.

## I. INTRODUCTION

In magnetic confinement of hot plasmas, anomalous transport leading to particle and heat loss is an important issue. Transport induced by drift wave turbulence has often been considered as a candidate for the anomalous transport.[1–3] On the other hand, it has been found that zonal flows can be excited by, and in turn suppress, the drift wave turbulence.[4–10] Zonal flow can have two branches, the low frequency zonal flow (LFZF) and the geodesic acoustic mode (GAM). The latter is characterized by finite oscillation frequency and poloidal asymmetry in the density perturbations. In tokamaks, due to the radial inhomogeneity of the plasma temperature, the oscillation frequency of the GAM is not constant along the minor radius.[11] The corresponding frequency continuum can be associated with unusual mode behavior. In this paper we analyze the frequency continuum, the evolution of the radial mode number $k_r(t)$, as well as the radial phase velocity of the GAM. It is found that the frequency continuum agrees well with the existing theory, as well as the evolution of the radial wave vector of the mode. It is also found that the radial phase velocity of the GAM is proportional to the ion thermal velocity, in agreement with the experimental observation.[20]

## II. SIMULATION

The simulation is carried out using the gyro-kinetic simulation code GTS for tokamaks.[12] As input we use the CMOD[13] experimental equilibrium data, with the magnetic field, temperature, and density profiles obtained using the ESC[14] and TRANSP[15] codes. The initial density profile $n_0(r)$ and temperature profile $T_i(r)$, $T_e(r)$ are shown in Fig. 1. The toroidal magnetic field on the magnetic axis is $B_0 = 5.8$T, the major radius is $R_0 = 0.67$m, and the minor radius is $a = 0.22$m. The simulation domain is from $r/a = 0.3$ to 0.9.

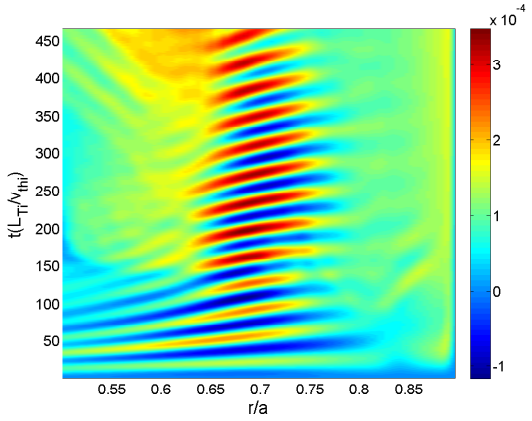


FIG. 2. (Color online.) Distribution of the radial electric field $E_r$.

Neoclassical effects such as that of the magnetic drift, etc. are included in the simulation.[16] Initially the particle velocities are assumed to be locally Maxwellian. Since the initial system is not in neoclassical equilibrium,[17] an oscillating but relatively homogeneous radial electric field $E_r$ is generated immediately after the simulation is started, as can be seen in Fig. 2 at small times.

One can see in Fig. 2 that the self-consistent evolution towards a neoclassical equilibrium triggers the oscillating electric field $E_r$. Then drift wave instabilities are excited in the region between $r/a = 0.6$ and 0.77, where the electron and ion temperature gradients are the largest (see Fig. 1(b)). The dominating ion-temperature-gradient (ITG) mode grows rapidly and the drift waves become turbulent. Simultaneously, the initial electric field oscillations become localized to the same radial region and greatly enhanced, appearing as characteristic GAM oscillations. In the process energy is transferred from the unstable and turbulent drift waves to the GAM until a balance is reached. The drift wave turbulence saturates at a level much lower than its peak value that occurred during the growth stage of the ITG instability. That is, except for the very early stage (since the starting systems are different), the development of the drift wave turbulence and GAM interaction is similar to the widely accepted scenario.[4–10]

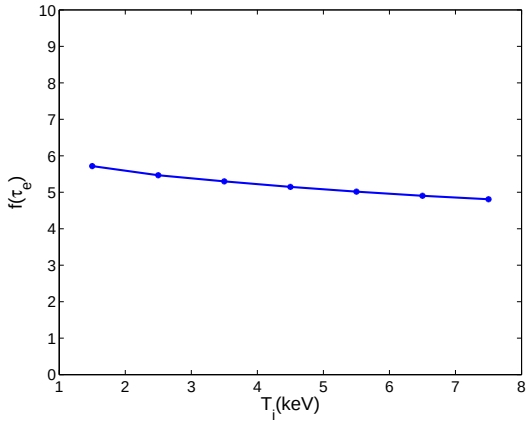


FIG. 3. (Color online.) Dependence of $f(\tau_e)$ on $T_i$ for $T_e = 4$keV and $q = 1.446$, as obtained from (1).

## III. FREQUENCY SPECTRUM

Accounting for the radial inhomogeneity of the plasma and neglecting nonlinear effects, one can express the GAM frequency as[18]

$$\omega_g = f(\tau_e)\frac{v_{thi}}{R_0 q}, \tag{1}$$

where $v_{thi} = \sqrt{T_i/m_i}$ is the ion thermal speed, $R_0$ is the major radius of the tokamak, and $q$ is the safety factor,

$$f(\tau_e) = \frac{\sqrt{(7+4\tau_e)}}{2} q \left[1 + \frac{2(23+16\tau_e+4\tau_e^2)}{q^2(7+4\tau_e)^2}\right]^{1/2},$$

and $\tau_e = T_e/T_i$ is the electron-to-ion temperature ratio. Fig. 3 shows that $f(\tau_e)$ is only weakly dependent on $T_i$. The frequency spectrum obtained from the simulation is shown in Fig. 4. One can clearly see the dominating GAM and the ITG excited drift-wave turbulence in the region between $r/a \sim 0.65$ and 0.75. One can also see a very-low and constant frequency regime between $r/a \sim 0.55$ and 0.7, which can be attributed to the LFZF.

As the ion temperature decreases outward along the minor radius, the GAM frequency also decreases. The frequencies obtained from the simulation and (1) are given in Fig. 5.

We see that in a small region the results from the simulation and theory agree quite well. The discrepancy in the other regions can be attributed to, among other reasons,[10] the fact that the GAM in the simulation is nonlinear (in fact, continuously interacting with the

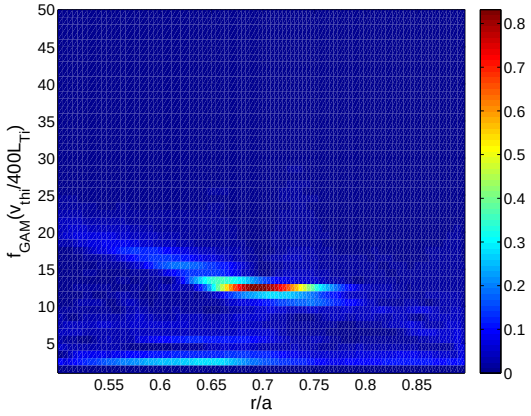


FIG. 4. (Color online.) Frequency spectrum of the GAM oscillations as obtained from the GTS simulations for the initial plasma configuration given in Fig. 1. The color code is for the relative mode strength.

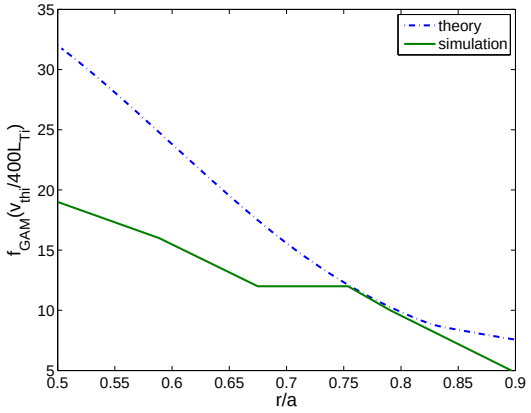


FIG. 5. (Color online.) Comparison of the GAM frequencies obtained from the simulation and theory. The disagreements at the smaller and large $r$ values can be attributed to nonlinear and boundary effects, respectively. Recall that the theory is linear and based on a collisionless model.

ITG-driven drift waves) and localized in a small region around $r/a \sim 0.7$, but the theory assumes that the GAM is linear and not radially localized.

## IV. THE RADIAL WAVE VECTOR $k_r$

Since the GAM frequency $\omega_g$ depends continuously on $r$, the local radial wave vector $k_r$ of the mode depends on time, i.e., $k_r = k_r(t)$, as can be seen in the evolution of the density

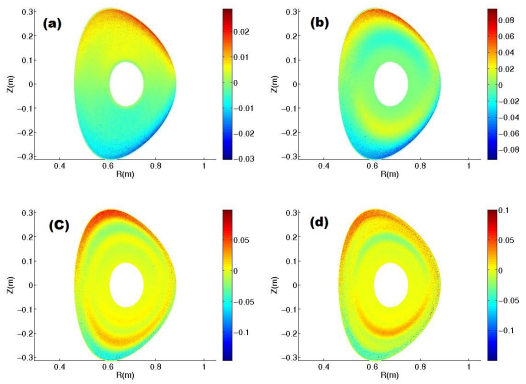


FIG. 6. (Color online.) (a)–(d) is the density perturbation $\delta n/n_0$ at $t$=5, 20, 35, 50 $L_{T_i}/v_{thi}$, respectively, on the (r,$\theta$) plane.

perturbation $\delta n/n_{00}$ shown in Fig. 6. Here $n_{00} = n_0(0.7a)$ and $\delta n \equiv n - n_0(r)$. We can see that the poloidal mode number is $m = 1$ and $k_r$ increases with time. To consider this property in more detail, we define the initial mode phase as[19]

$$\phi = \omega_g(r)t - k_0 r + \phi_0. \tag{2}$$

As shown in Fig. 7, the initial mode vector $k_0 \approx 0$, so that

$$k_r = -\frac{d\phi}{dr} = -\frac{d\omega_g(r)}{dr}t, \tag{3}$$

$$\frac{dk_r}{dt} = -\frac{d\omega_g(r)}{dr}. \tag{4}$$

The evolution of the radial wave vector $k_r$ is shown in Fig. 7. One can see that it increases with time, and the trend is indicated by the black line in the figure. To calculate $dk_r/dt$, we make use of the end points of this line, namely $\Delta k_r = 10\pi/0.4a$, $\Delta t = 80L_{T_i}/v_{thi}$, so that the averaged value of $dk_r/dt$ is $\Delta k_r/\Delta t = 0.98v_{thi}/aL_{T_i}$. The averaged $d\omega_g/dr$ given by $\Delta\omega_g/\Delta r$, where $\Delta r = 0.4a$ and $\Delta\omega_g$ is the frequency difference between $r/a = 0.5$ and 0.9. Thus, the theoretical value is $\Delta\omega_g/\Delta r = -1.06v_{thi}/aL_{T_i}$, which agrees well with that (obtained by evaluating the slope $dk_r/dt$ of the black line in Fig. 7) from the simulation.

## V. RADIAL PROPAGATION CHARACTERISTICS

The radial propagation of the GAM has been considered in several works.[20–22] Accordingly, we consider the effect of $n_0$ for $T_i$ = 6keV, $T_e$ = 4keV, $R_0/L_{T_i}$ = 2.4 and

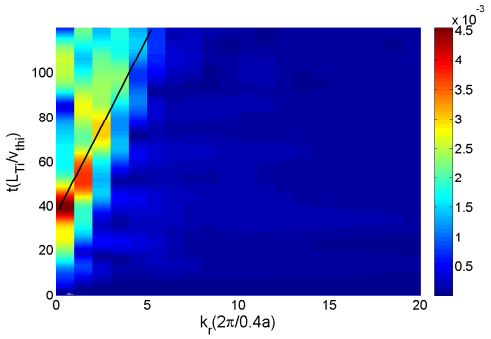


FIG. 7. (Color online.) Evolution of the radial wave vector $k_r(t)$ of the GAM.

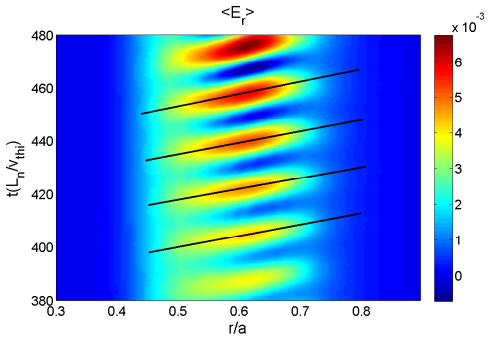


FIG. 8. (Color online.) The radial velocity $v_r$.

$R_0/L_n = R_0/L_{T_e} = 6$. From the four lines marking the peaks of the mode in Fig. 8, one can obtain (from their averaged gradient) the mean radial velocity of the GAM. The result is shown in Fig. 9, where $v_{thi0}$ is the thermal velocity of deuteron for $T_i = 6$keV. One can see that $v_r$ is almost independent of $n_0$. This result differs from that of a TEXTOR experiment,[20] which finds that $v_r$ decreases with increase of the local plasma density. The discrepancy can be attributed to the fact in our GTS simulation the collision frequency is fixed and the temperature range is considerably higher than that in the experiment. Instead, our simulation shows that the radial GAM velocity depends linearly on the ion thermal speed, namely $v_r \sim 0.05 v_{thi}$.

Accordingly, we have also separately investigated the effects of $T_i$ and $m_i$, keeping the other parameters fixed. In Fig. 10 for $v_r$ versus $T_i$ we see that $v_r/v_{thi0} \sim 0.061$ at $T_i = 6$keV, which agrees well with the value in Fig. 9. To further confirm our result, Fig. 11 for $v_r$ versus $m_i$ shows that $v_r/v_{thi0} \sim 0.04515$ for $m_i = m_D$, which is also consistent with that from Figs. 9 and 10. The result for $v_r$ versus $T_i$ from Ref. 20 is shown in Fig. 12. We see that it is consistent with that in Fig. 10. The ratio $v_r/v_{thi} \sim 0.0387$ is also quite close that

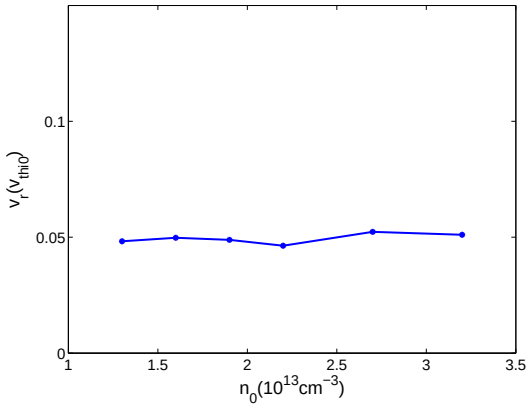


FIG. 9. (Color online.) $v_r$ versus $n_0$. Here, $v_{thi0}$ is the thermal velocity of deuteron for $T_i = 6$keV.

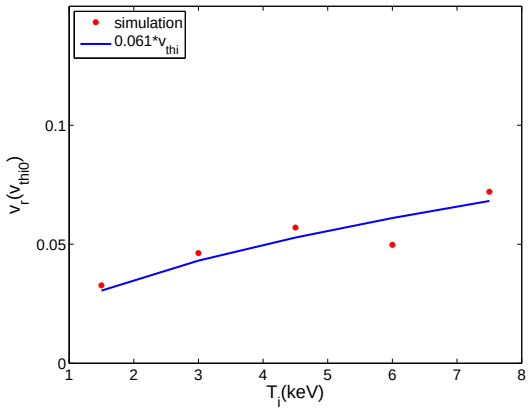


FIG. 10. (Color online.) $V_r$ versus $T_i$.

found in our simulation.

These relations can be expected: In terms of the GAM wavelength $\lambda = 2\pi/k_r$, the radial phase velocity of the GAM is $v_r = \lambda f(\tau_e) v_{thi}/2\pi R_0 q$. As shown in Fig. 3, in the regime of interest $f(\tau_e)$ depends only weakly on $T_i$. The wavelength $\lambda$ of the GAM should roughly be the width of GAM-drift wave interaction region along the minor radius. One can see from Fig. 8 that $\lambda \sim 0.3a$. Thus, we have $v_r = 0.05 v_{thi}$, in agreement with the simulation result. Accordingly, one can conclude that $v_r$ depends linearly on $v_{thi}$.

## VI. SUMMARY

In this paper, the frequency continuum, the $k_r$ evolution, and the radial phase velocity of the GAM have been investigated using GTS simulation and a simple analytical model. The

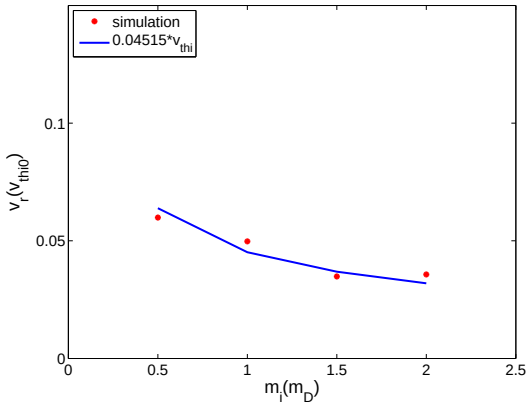


FIG. 11. (Color online.) $v_r$ versus the ion mass $m_i$, where $m_D$ is the mass of Deuteron.

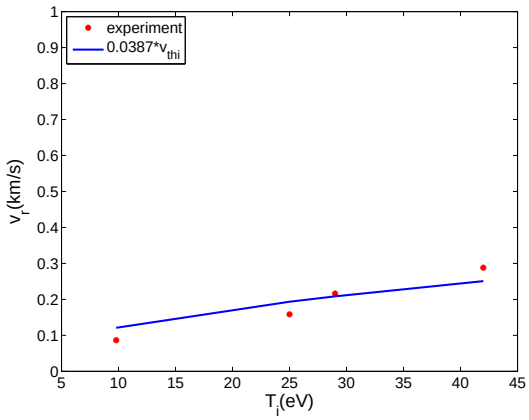


FIG. 12. (Color online.) $v_r$ versus $T_i$ from the experiment in 20 for $T_e \sim T_i$.

frequency continuum agrees quite well with that from the model. The evolution of $k_r$ and the radial propagation of the GAM are numerically simulated and it is found that the phase velocity of the mode is proportional to the ion thermal velocity, in fact $v_r/v_{thi} \approx 0.05$. These results are in agreement with that from the TEXTOR experiments.[20] However, the density dependence of the GAM frequency found in the latter is not recovered in our simulation, since we could not fully implement the experimental conditions in our simulation code. We note that the results here may also be applicable to other zonal flows, such as that in the Earth's upper atmosphere.[23]

## ACKNOWLEDGMENTS

We would like to thank Zhiyong Qiu for useful discussions. This work has been supported by the National Magnetic Confinement Fusion Program under Grant No. 2013GB104004, the National Natural Science Foundation of China (NSFC) under Grant No. 11235009, and Fundamental Research Fund for Chinese Central Universities under Grant No. 2016FZA3003.

## REFERENCES

[1]J. Callen, Phys. Rev. Lett. **39**, 1540 (1977).

[2]W. Horton, Rev. Mod. Phys. **71**, 735 (1999).

[3]Y. Xiao, I. Holod, W. Zhang, S. Klasky, and Z. Lin, Phys. Plasmas **17**, 022302 (2010).

[4]Z. Lin, T. S. Hahm, W. Lee, W. M. Tang, and R. B. White, Science **281**, 1835 (1998).

[5]S. Coda, M. Porkolab, and K. H. Burrell, Phys. Lett. A **273**, 125 (2000).

[6]J. Anderson, H. Nordman, R. Singh, and J. Weiland, Phys. Plasmas **9**, 4500 (2002).

[7]P. H. Diamond, S. I. Itoh, K. Itoh, and T. S. Hahm, Plasma Phys. Control. Fusion **47**, R35 (2005).

[8]T. Kaladze, D. Wu, O. Pokhotelov, R. Sagdeev, L. Stenflo, and P. K. Shukla, Phys. Plasmas **12**, 122311 (2005).

[9]T. Lan, A. D. Liu, C. X. Yu, L. W. Yan, W. Y. Hong, K. J. Zhao, J. Q. Dong, J. Qian, J. Cheng, D. L. Yu, and Q. W. Yang, Phys. Plasmas **15**, 056105 (2008).

[10]Z. Qiu, L. Chen, and F. Zonca, Phys. Plasmas **21**, 022304, (2014).

[11]N. Winsor, J. L. Johnson, and J. M. Dawson, Phys. Fluids **11**, 2448 (1968).

[12]W. X. Wang, Z. Lin, W. M. Tang, W. W. Lee, S. Ethier, J. L. V. Lewandowski, G. Rewoldt, T. S. Hahm, and J. Manickam, Phys. Plasmas **13**, 092505 (2006).

[13]I. H. Hutchinson, R. Boivin, F. Bombarda, P. Bonoli, S. Fairfax, C. Fiore, J. Goetz, S. Golovato, R. Granetz, M. Greenwald, et al., Phys.Plasmas **1**, 1511 (1994).

[14]L. E. Zakharov and A. Pletzer, Phys. Plasmas **6**, 4693 (1999).

[15]R. J. Goldston, D. C. McCune, H. H. Towner, S. Davis, R. J. Hawryluk, and G. L. Schmidt, J. Comput. Phys. **43**, 61 (1981).

[16]W. X. Wang, S. Ethier, Y. Ren, S. Kaye, J. Chen, E. Startsev, Z. Lu, and Z. Q. Li, Phys. Plasmas **22**, 102509 (2015).

[17]S. V. Novakovskii, C. S. Liu, R. Z. Sagdeev, and M. N. Rosenbluth, Phys. Plasmas **4**, 4272 (1997).

[18]H. Sugama and T.-H. Watanabe, J. Plasma Phys. **72**, 825 (2006).

[19]Z. Qiu, *Theories of Geodesic Acoustic Modes in Tokamak Plasmas* (Ph.D. dissertation, University of Science and Technology of China, Hefei, China, 2010).

[20]Y. Xu, I. Shesterikov, M. Van Schoor, M. Vergote, R. Weynants, A. Krämer-Flecken, S. Zoletnik, S. Soldatov, D. Reiser, K. Hallatschek, et al., Plasma Phys. Control. Fusion **53**, 095015 (2011).

[21]T. Lan, A. D. Liu, C. X. Yu, L. W. Yan, W. Y. Hong, K. J. Zhao, J. Q. Dong, J. Qian, J. Cheng, D. L. Yu, et al., Plasma Phys. Control. Fusion **50**, 045002 (2008).

[22]Z. Qiu, F. Zonca, and L. Chen, Plasma Sci. Technol. **13**, 257 (2011).

[23]T. Kaladze, O. Pokhotelov, L. Stenflo, J. Rogava, L. Tsamalashvili, and M. Tsiklauri, Phys. Lett. A **372**, 5177 (2008).